

Figure 1. Structure and UV/visible spectrum of rotenone.

Actonick donated this figure.

Table 23. Comparative adsorption and desorption of sterilized and unsterilized sediments at pH 7.

Sediment source	Adsorption ($\mu\text{g/g}$)		Desorption (%)	
	Unsterile	Sterile	Unsterile	Sterile
Mississippi River (RM 707)	0	0	--	--
Mississippi River (RM 704)	9.21	9.16	2.7	2.9
Arkansas	7.73	7.66	10.4	9.5
Chocolay River	8.69	8.75	2.7	3.2
Ford River	8.37	8.43	21.9	4.4

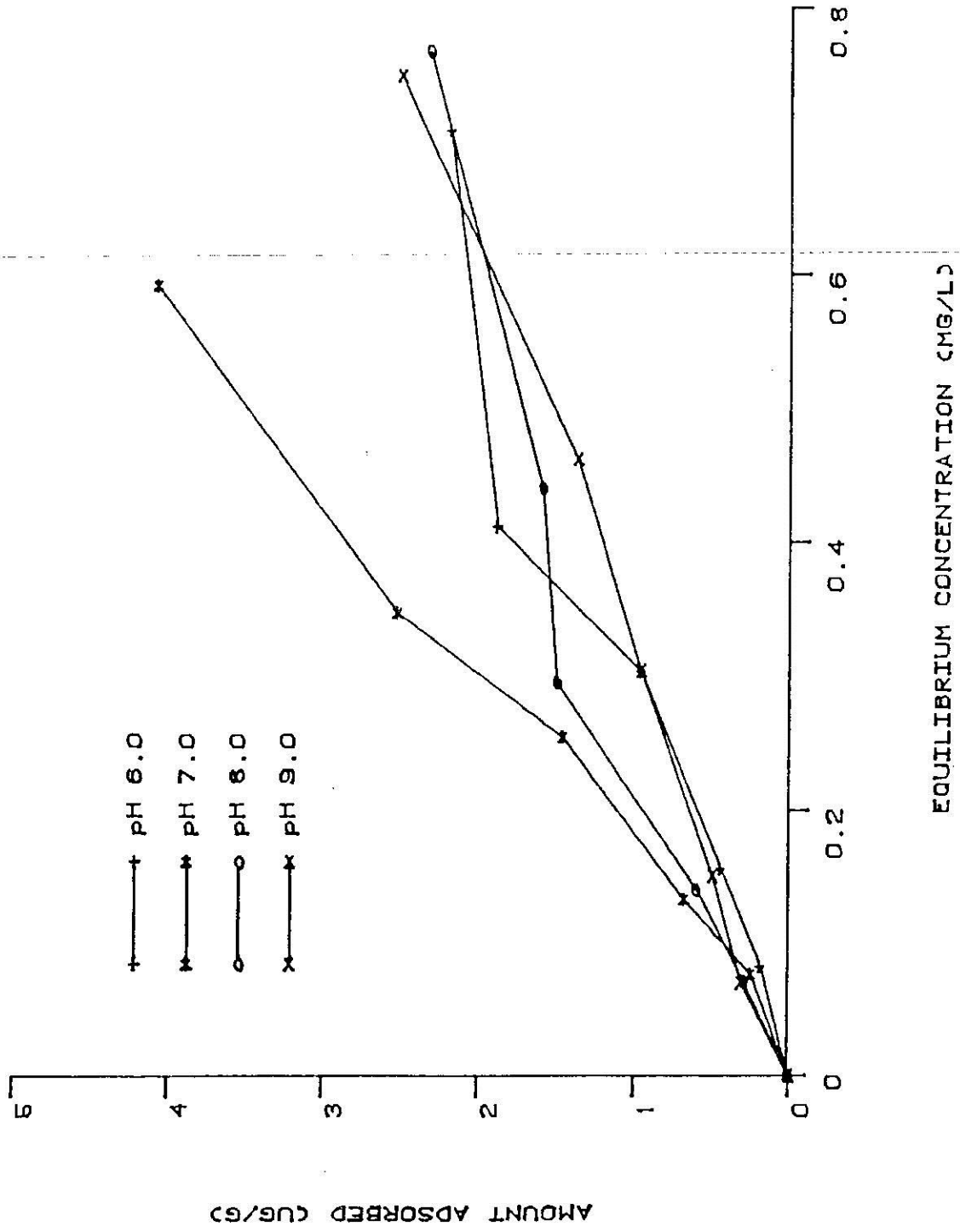


Figure 2. Adsorption equilibria for ^{14}C -rotenone by sediments from the Mississippi River main channel (River mile 707) at 5°C and four pH's.

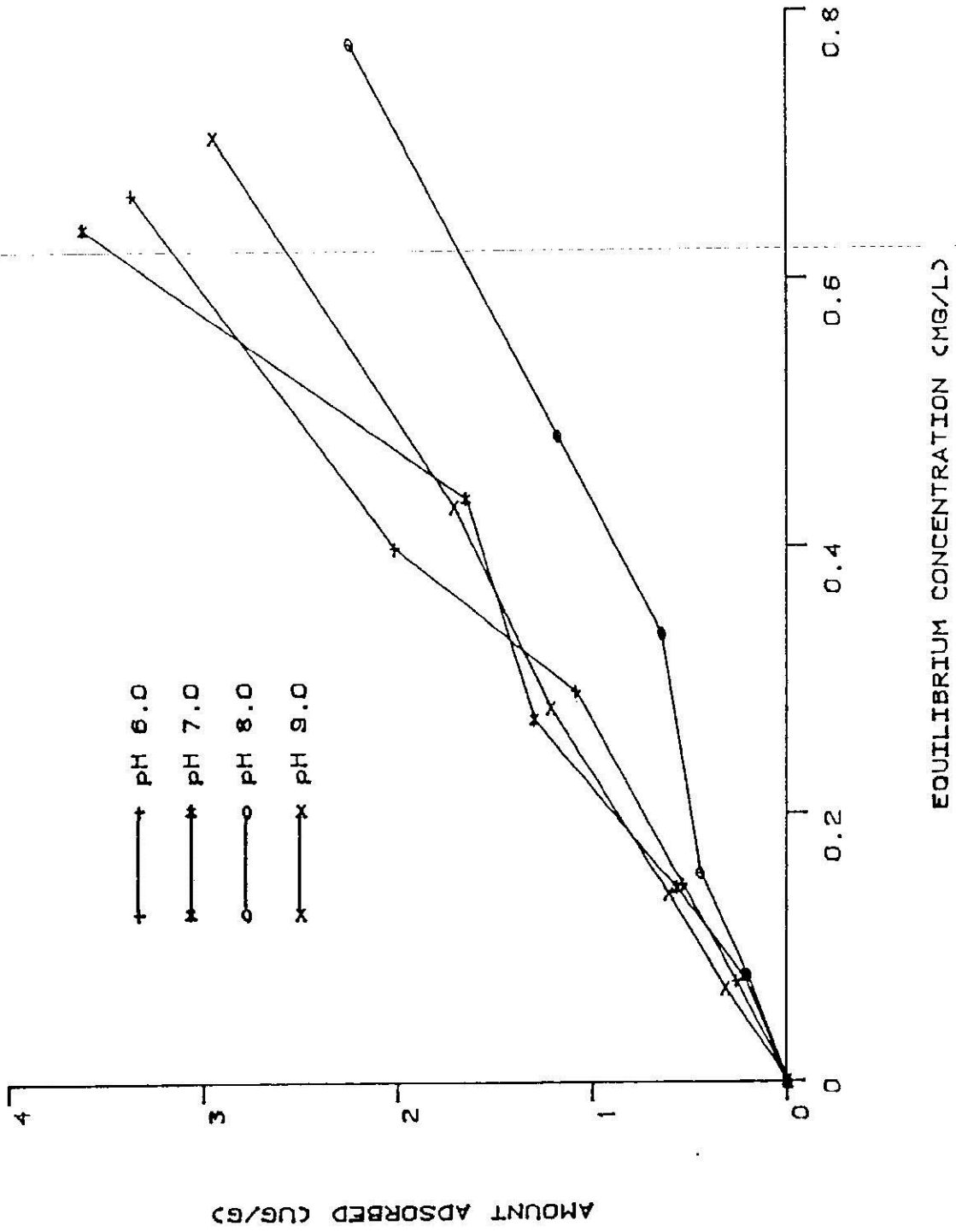


Figure 3. Adsorption equilibrium for ¹⁴C-rotenone by sediments from the Mississippi River main channel (River mile 707) at 20°C and four pH's.

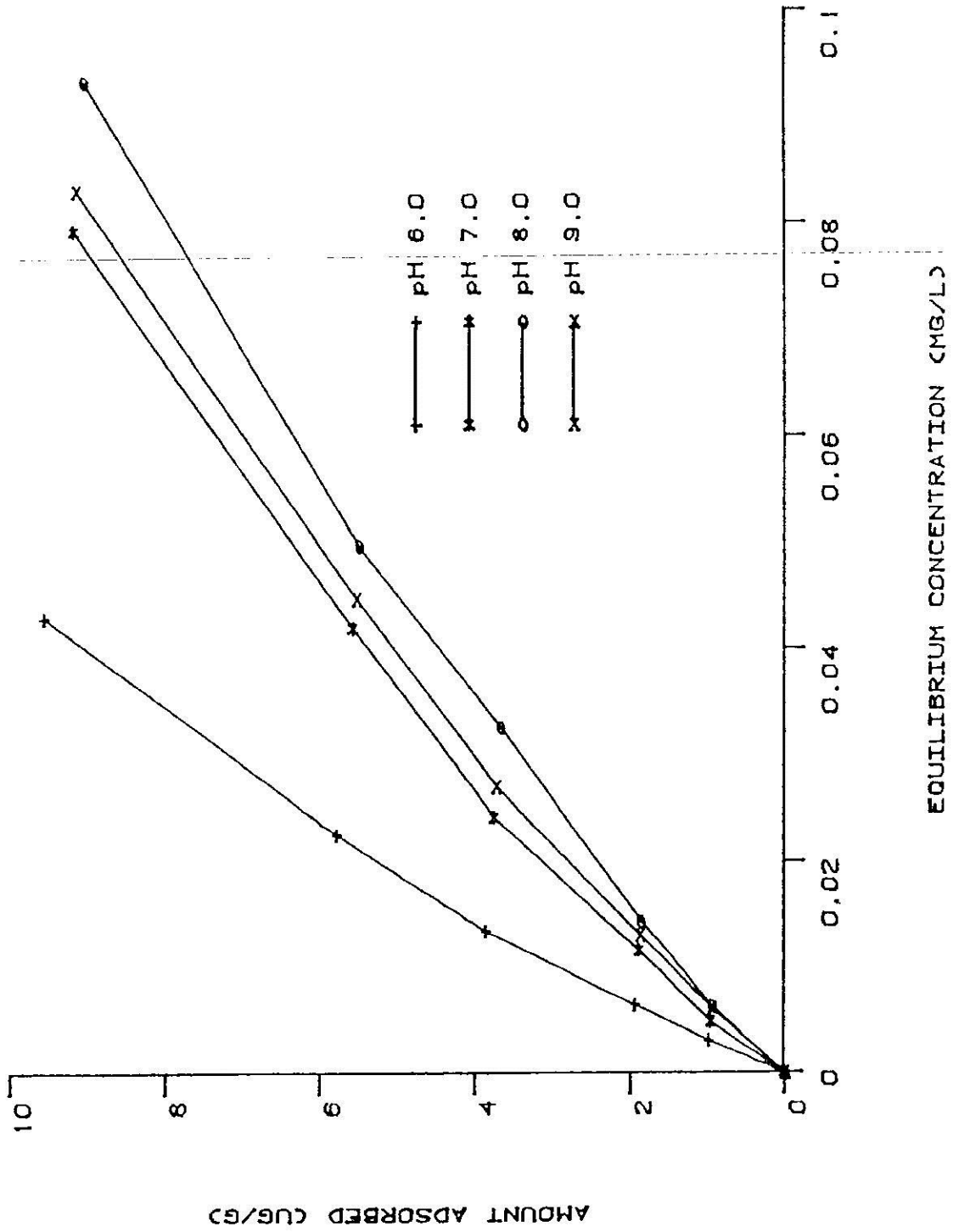


Figure 4. Adsorption equilibria for ¹⁴C-rotenone by sediments from the Mississippi River backwater (River mile 704) at 5°C and four pH's.

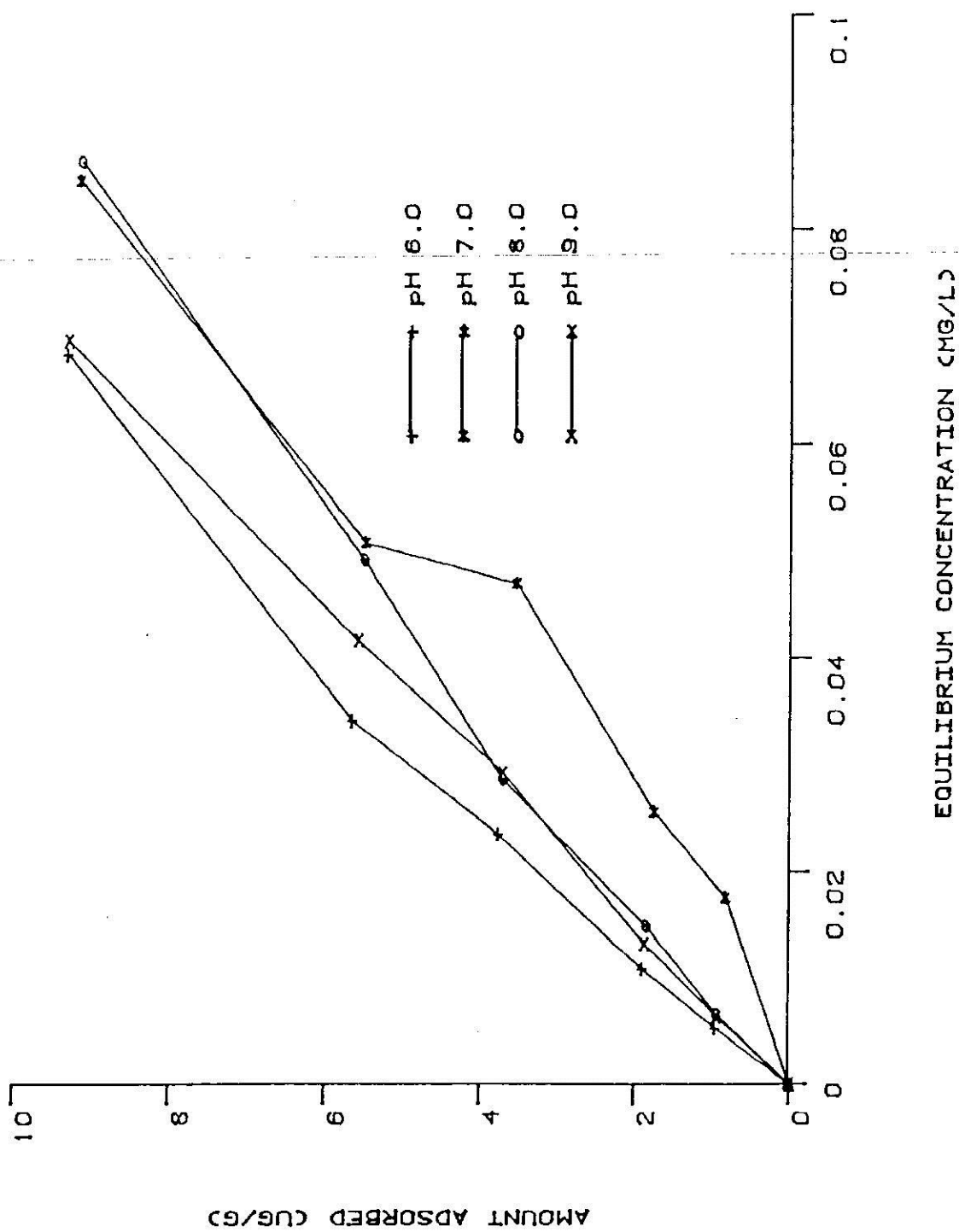


Figure 5. Adsorption equilibrium for ^{14}C -rotenone by sediments from the Mississippi River backwater (River number 704) at 20°C and four pH's.

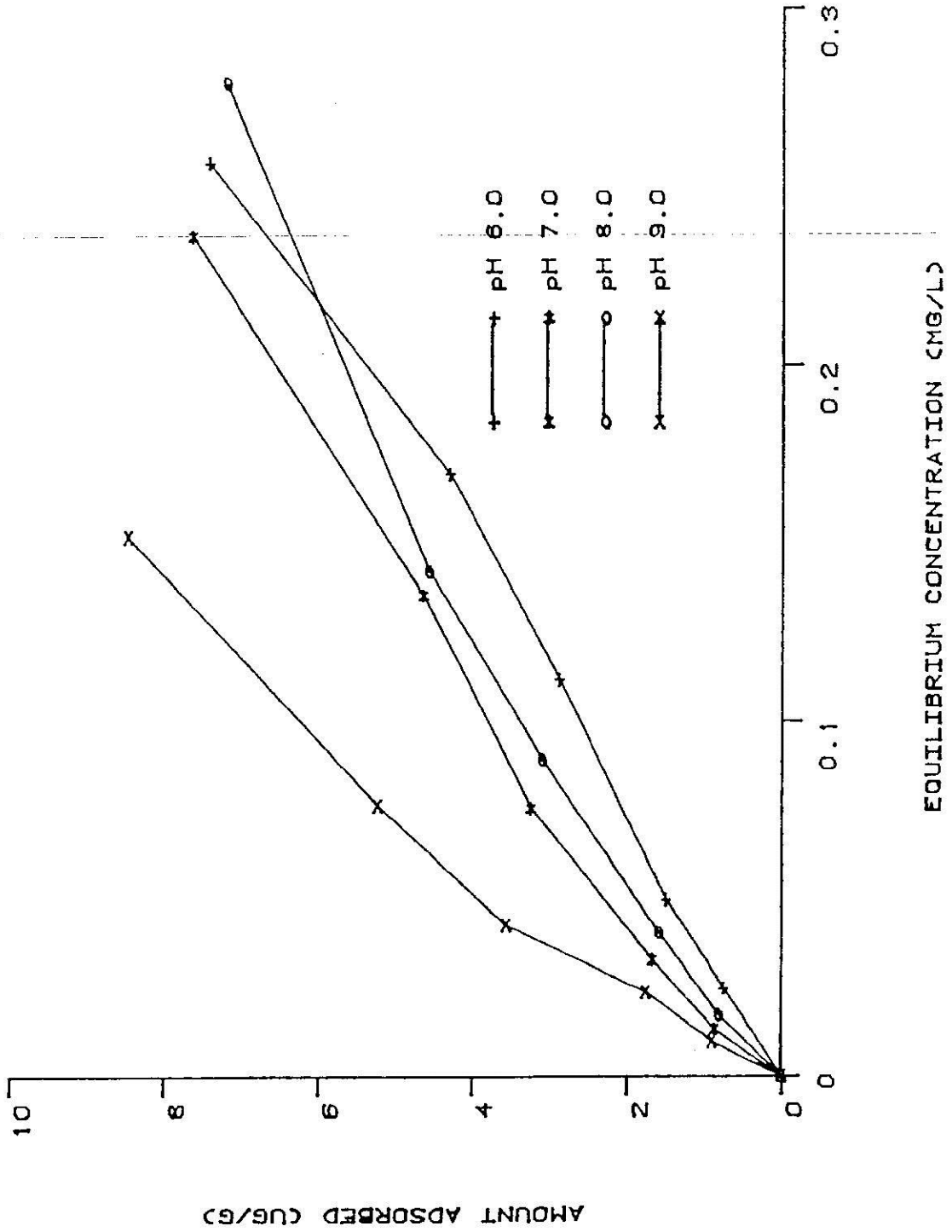


Figure 6. Adsorption equilibria for ¹⁴C-rotenone by sediments from the Rice Branch Experiment Station, Arkansas, at 5°C and four pH's.

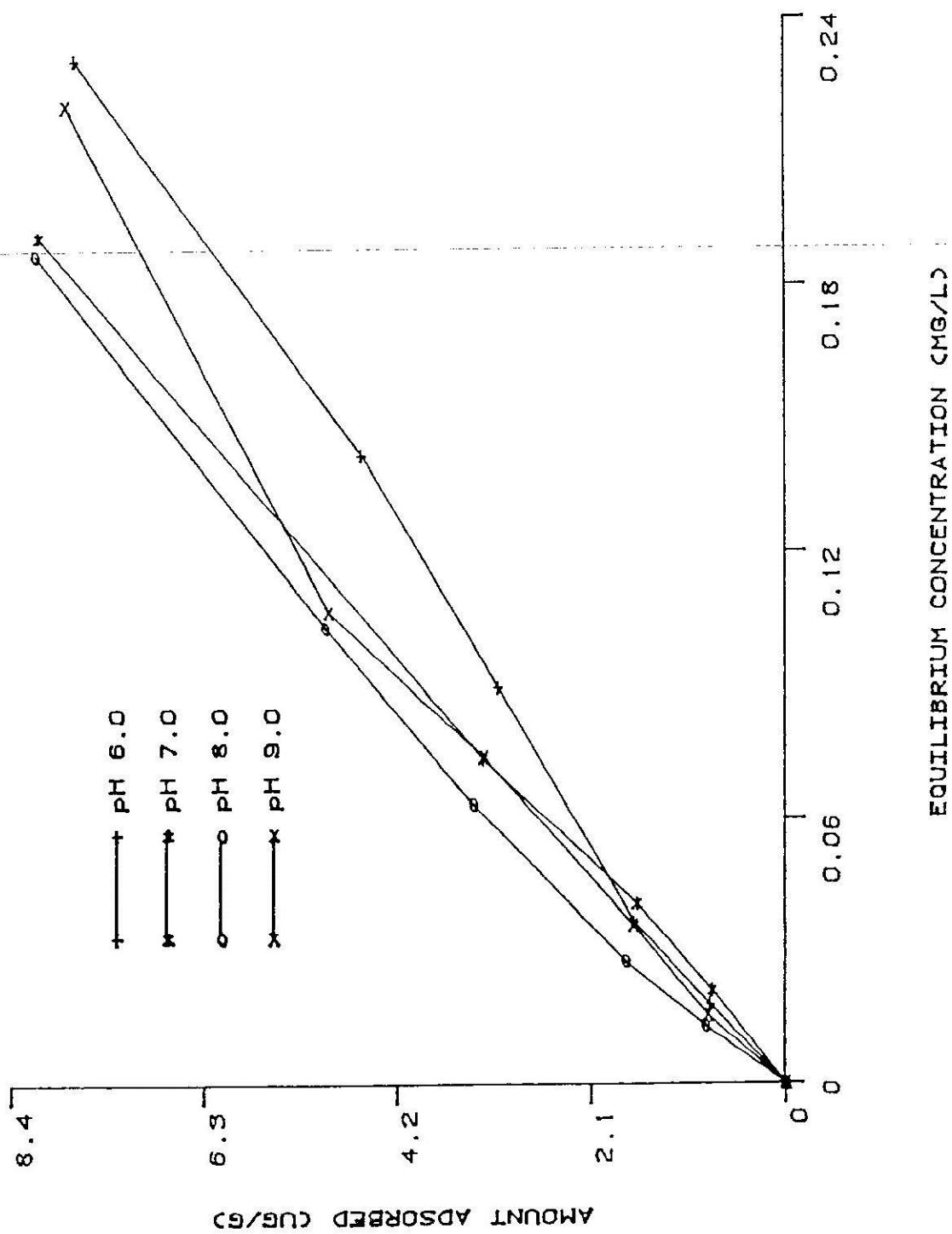


Figure 7. Adsorption equilibrium for ^{14}C -rotenone by sediments from the Rice Branch Experiment Station, Arkansas at 20°C and four pH's.

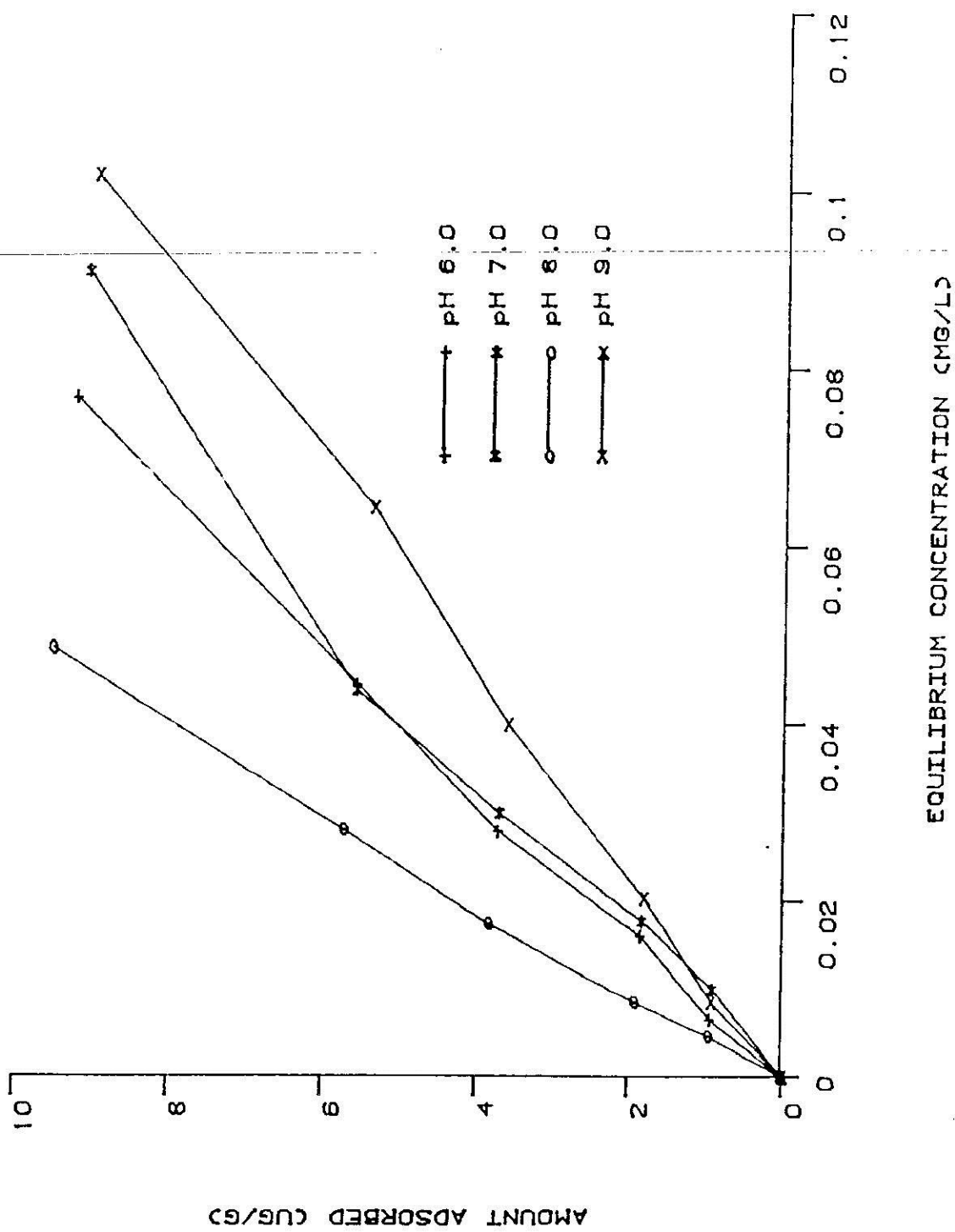


Figure 8. Adsorption equilibria for ¹⁴C-rotenone by sediments from the Chocollay River, Michigan, at 5°C and four pH's.

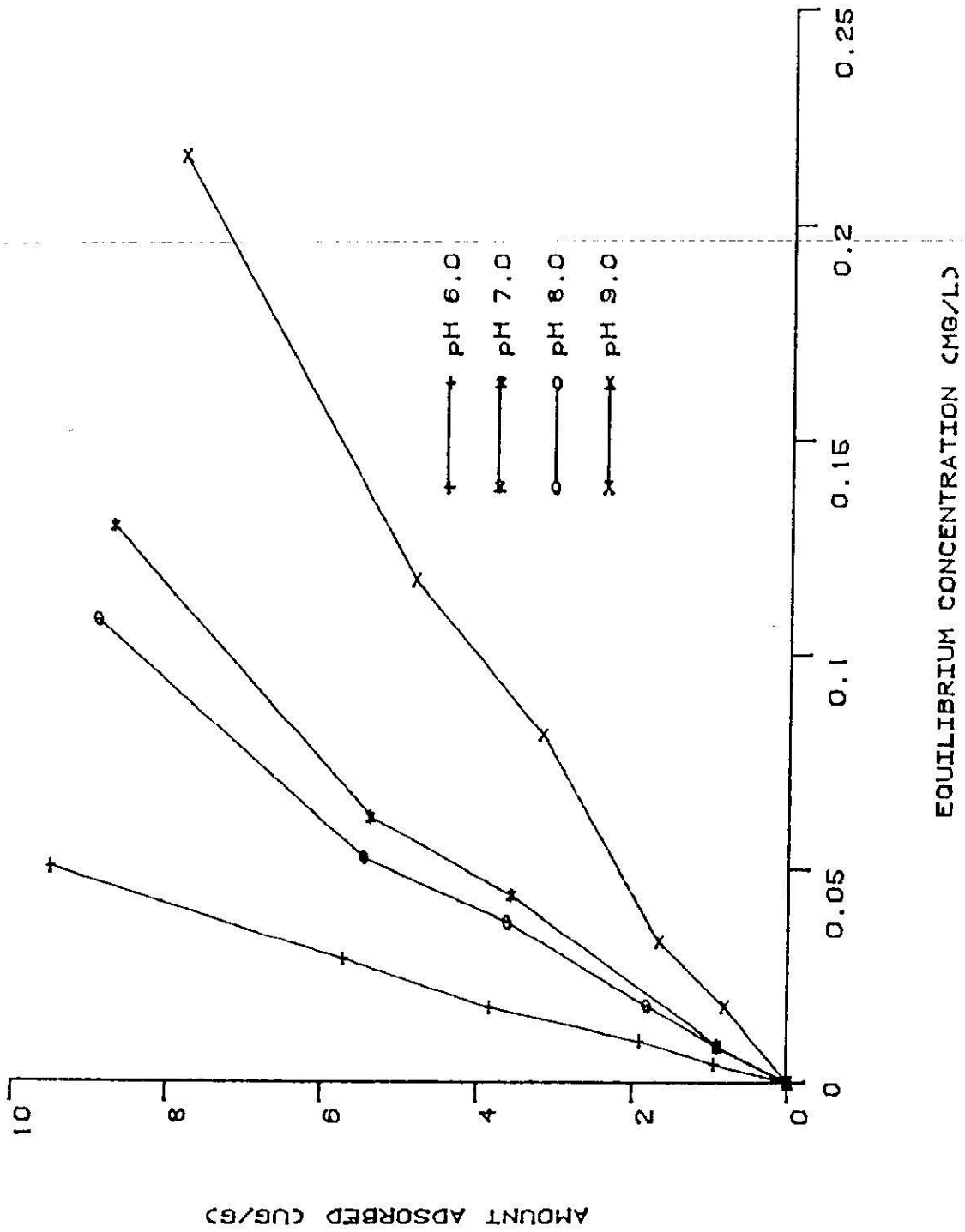


Figure 9. Adsorption equilibria for ¹⁴C-rotenone by sediments from the Choccolay River, Michigan, at 20°C for four pH's.

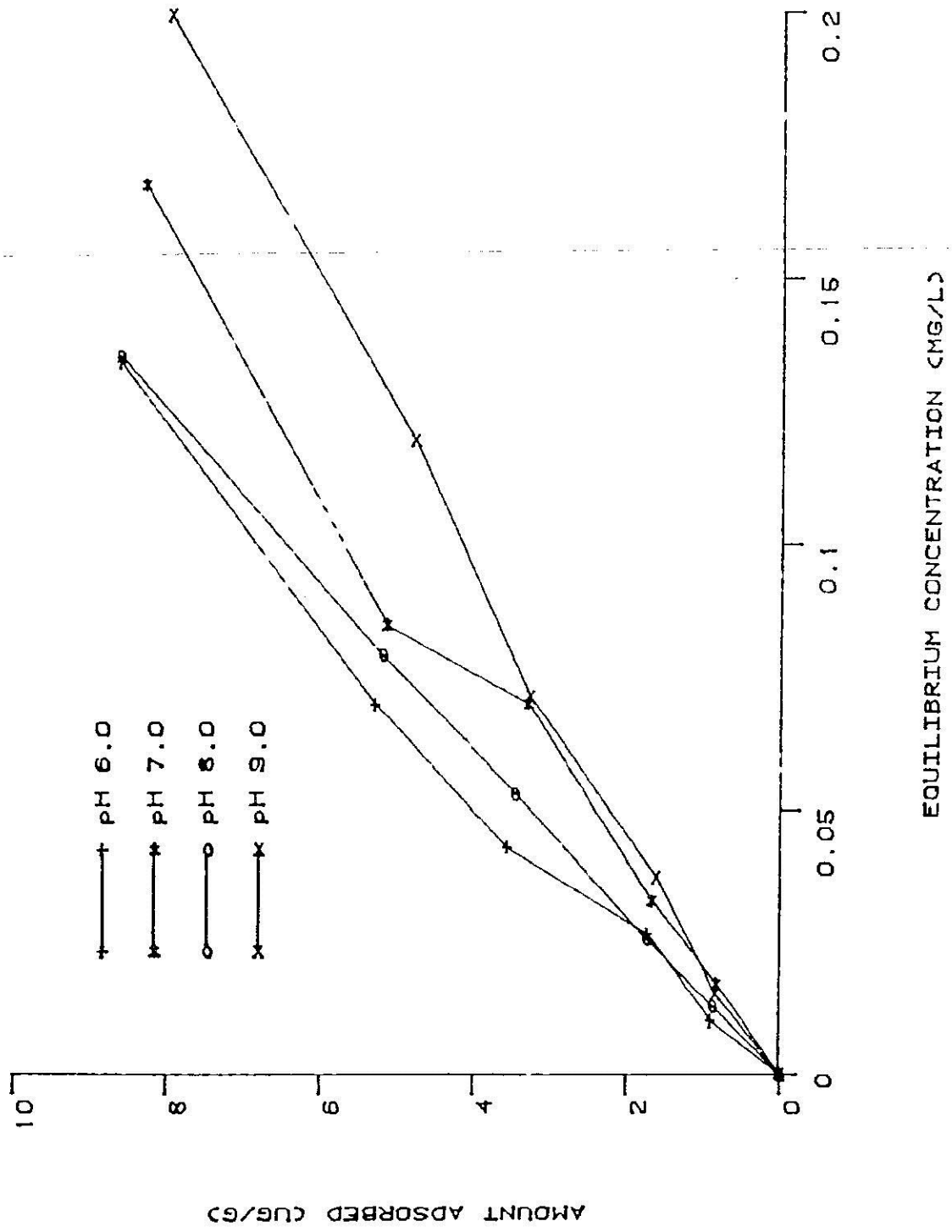


Figure 10. Adsorption equilibria for ¹⁴C-rotenone by sediments from the Ford River, Michigan, at 5°C and four pH's.

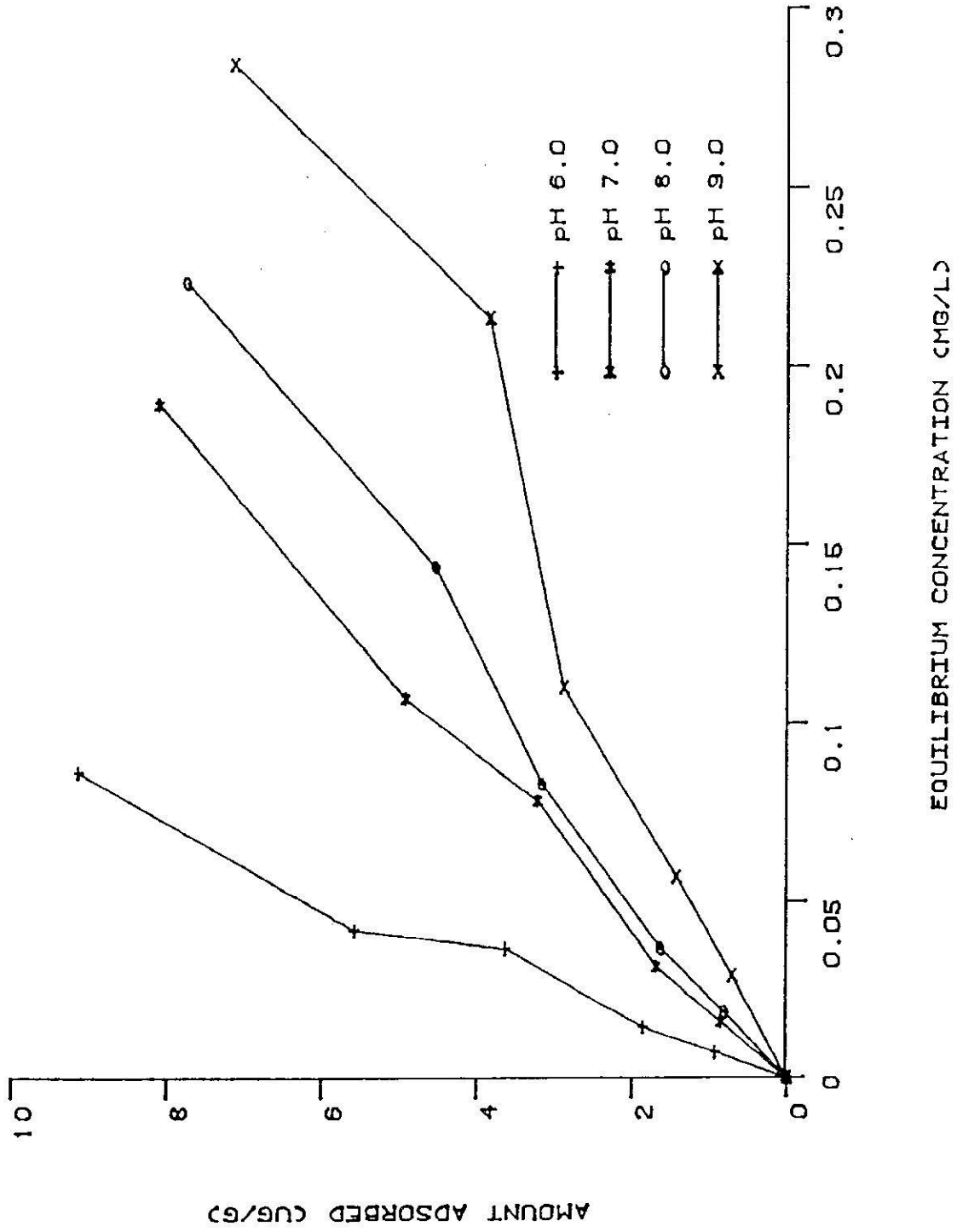


Figure 11. Adsorption equilibria for ¹⁴C-rotenone by sediments from the Ford River, Michigan, at 20°C and four pH's.

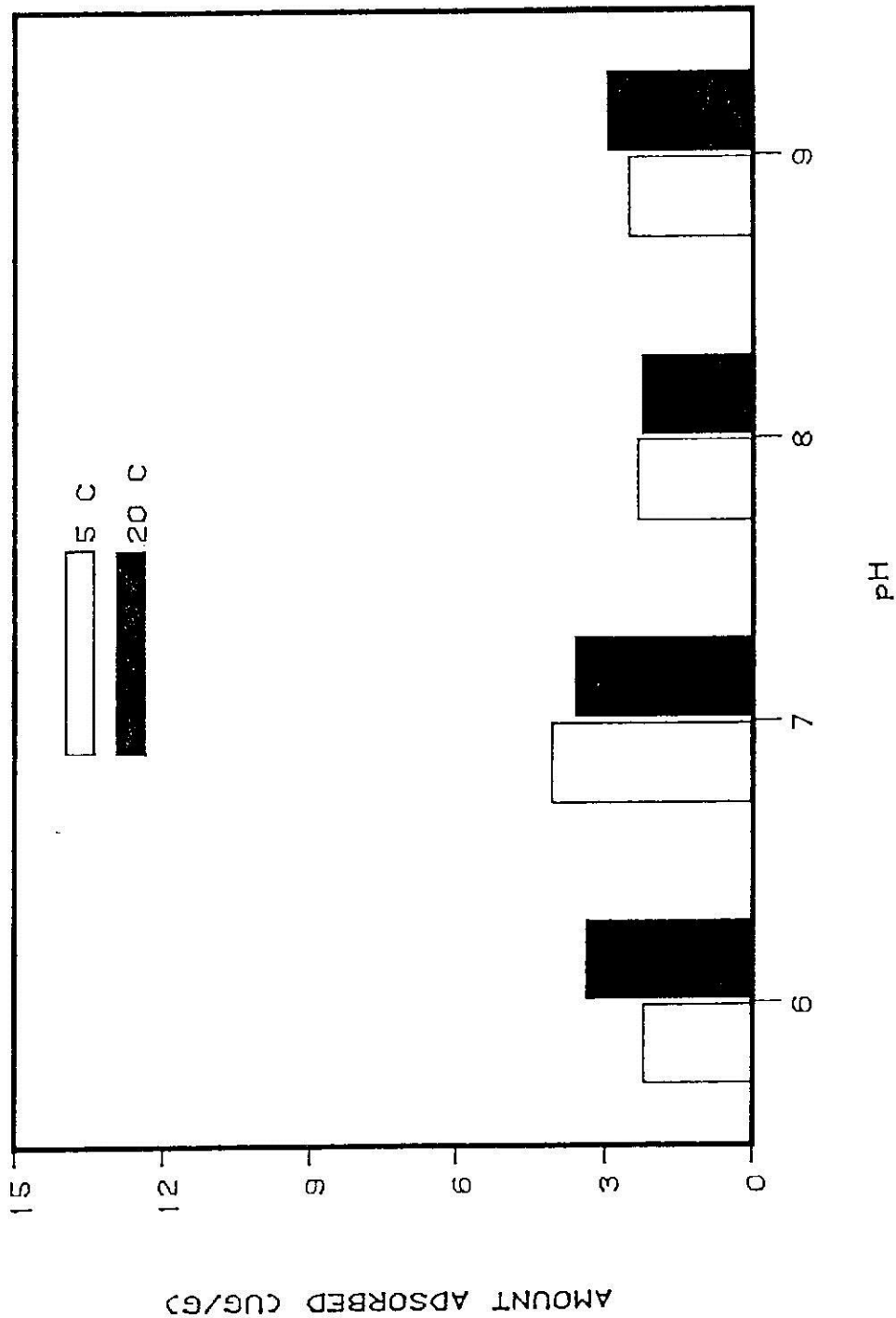


Figure 12. Adsorption of 1 mg/L solutions of ¹⁴C-rotenone on Mississippi River main channel (River mile 707) sediments at selected temperatures and pH's.

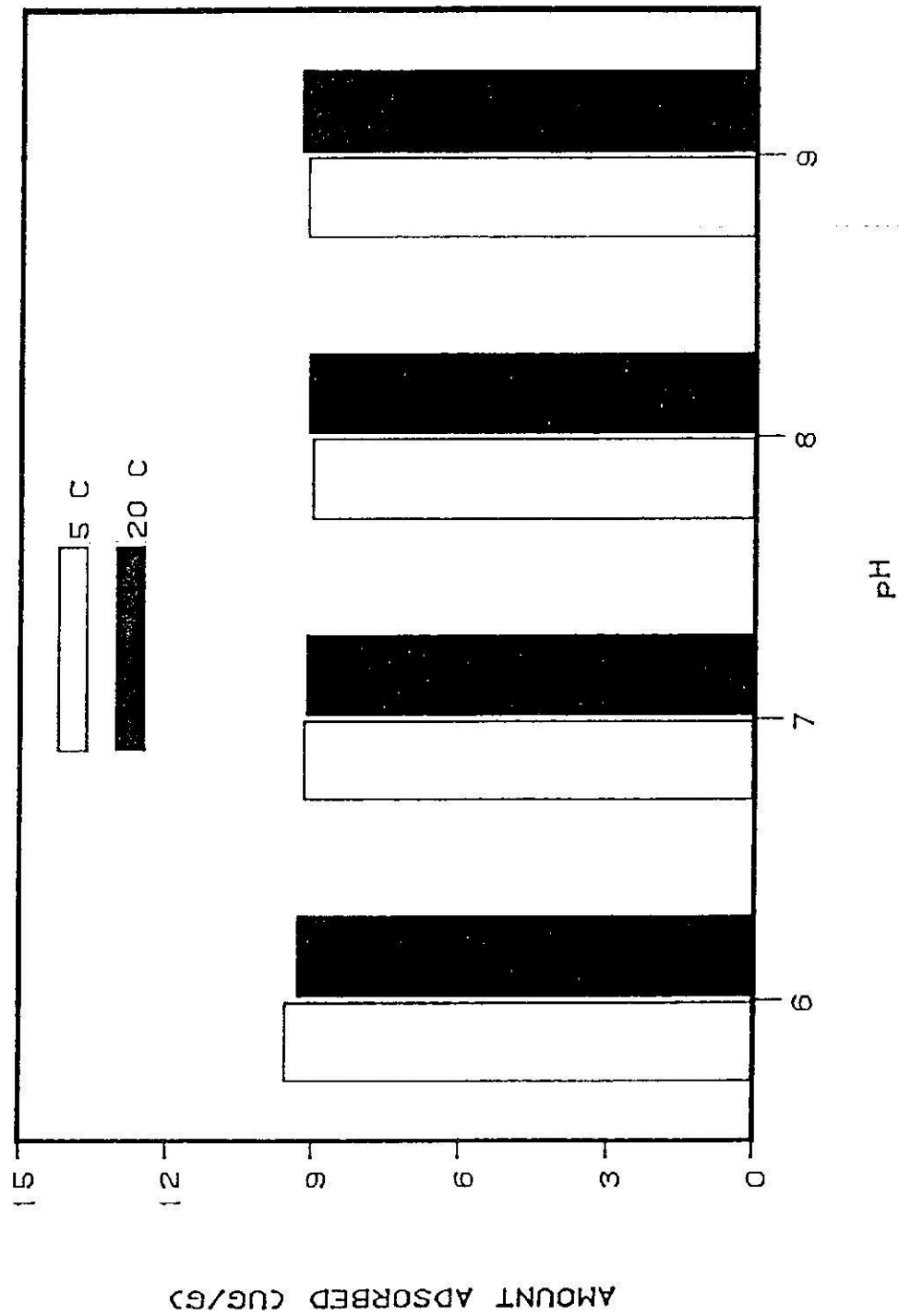


Figure 13. Adsorption of 1 mg/L solutions of ¹⁴C-rotenone on Mississippi River backwater (River mile 704) sediments at selected temperatures and pH's.

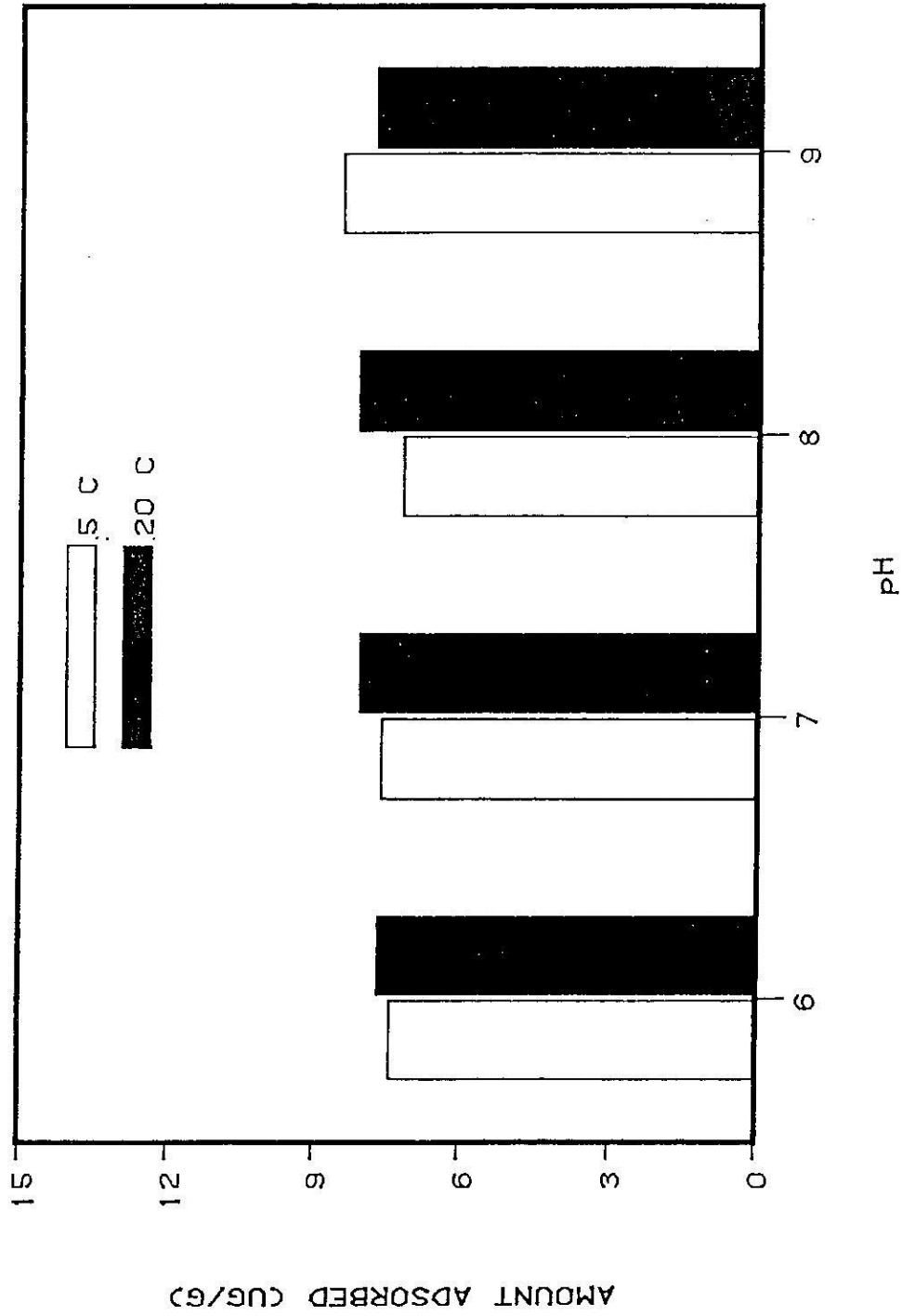


Figure 14. Adsorption of 1 mg/L solutions of ¹⁴C-rotenone on Rice Branch Experiment Station, Arkansas, sediments at selected temperatures and pH's.

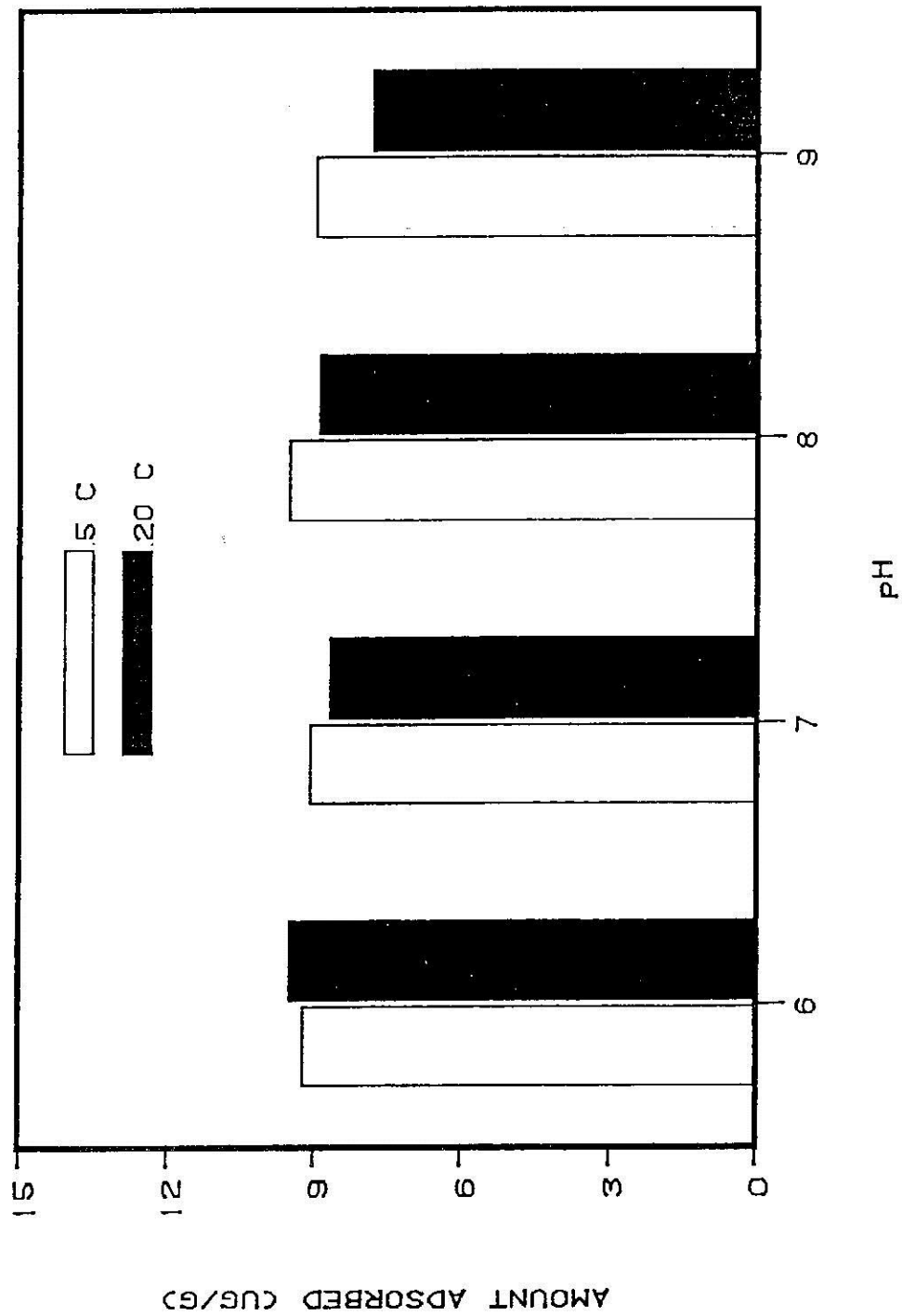


Figure 15. Adsorption of 1 mg/L solutions of ¹⁴C-rotenone on Chocolay River, Michigan, sediments at selected temperatures and pH's.

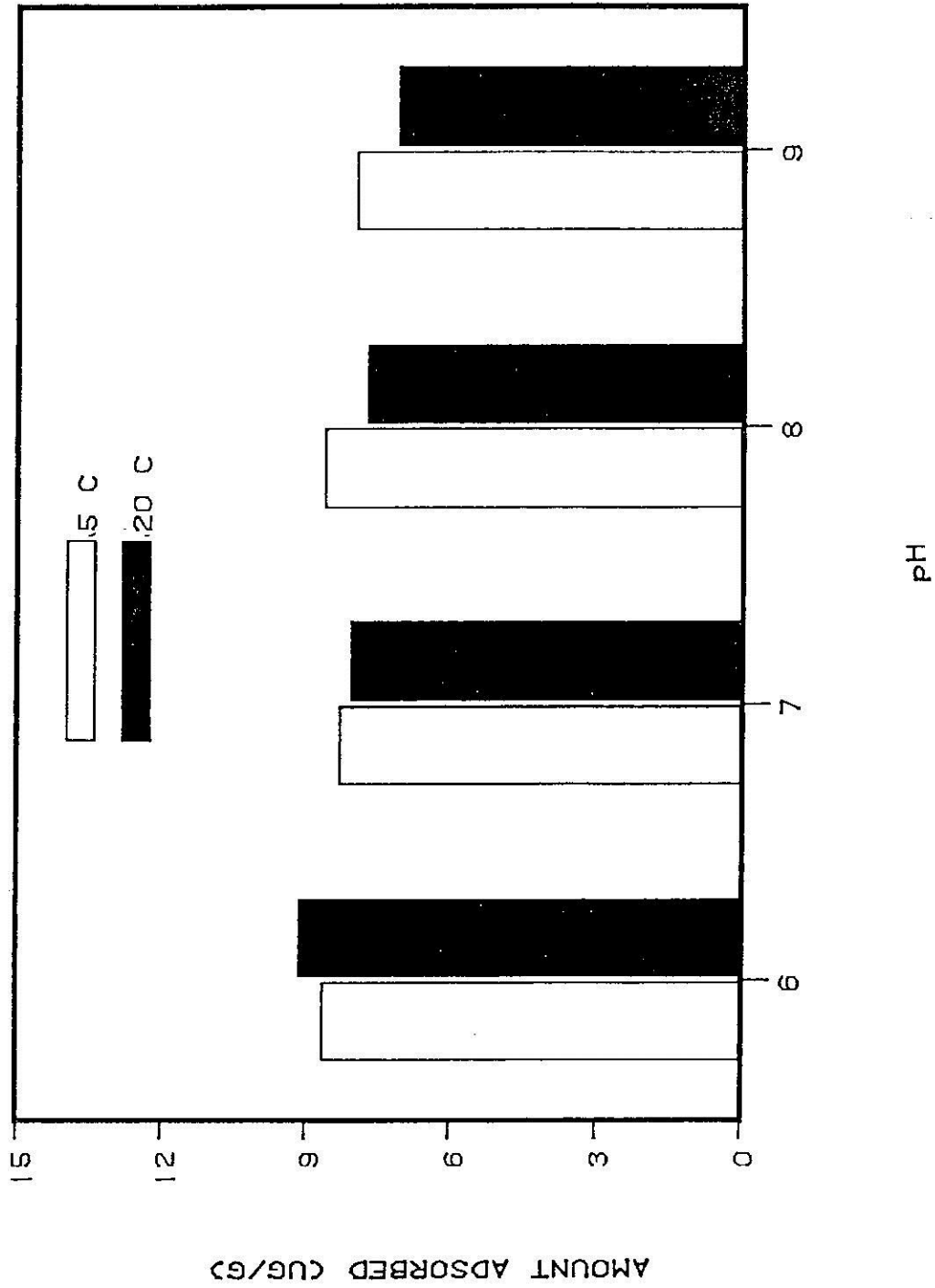


Figure 16. Adsorption of 1 mg/L solutions of ¹⁴C-rotenone on Ford River, Michigan, sediments at selected temperatures and pH's.

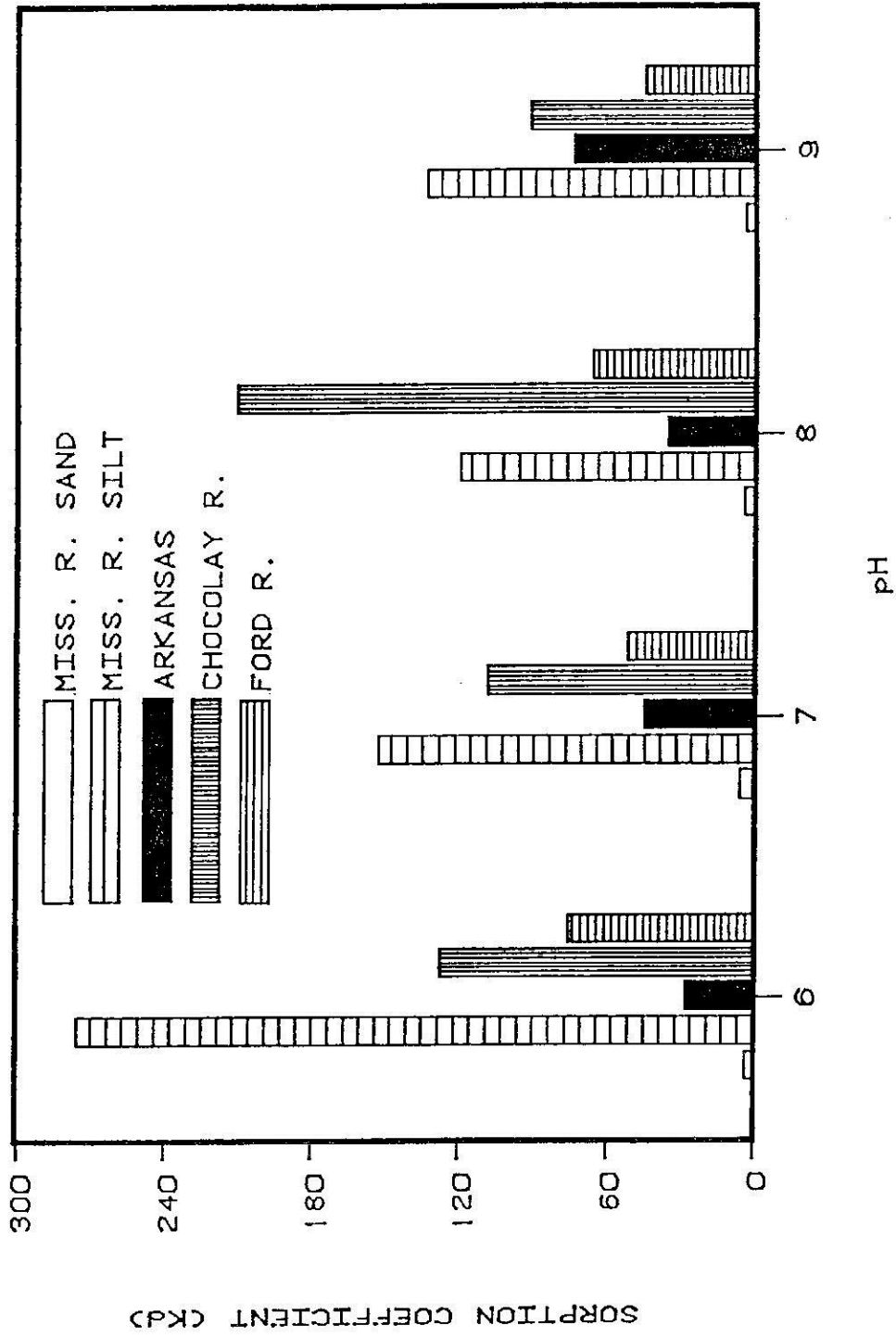


Figure 17. Sorption coefficients (K_d) for ^{14}C -rotenone by five different sediments at four pH's and 5°C .

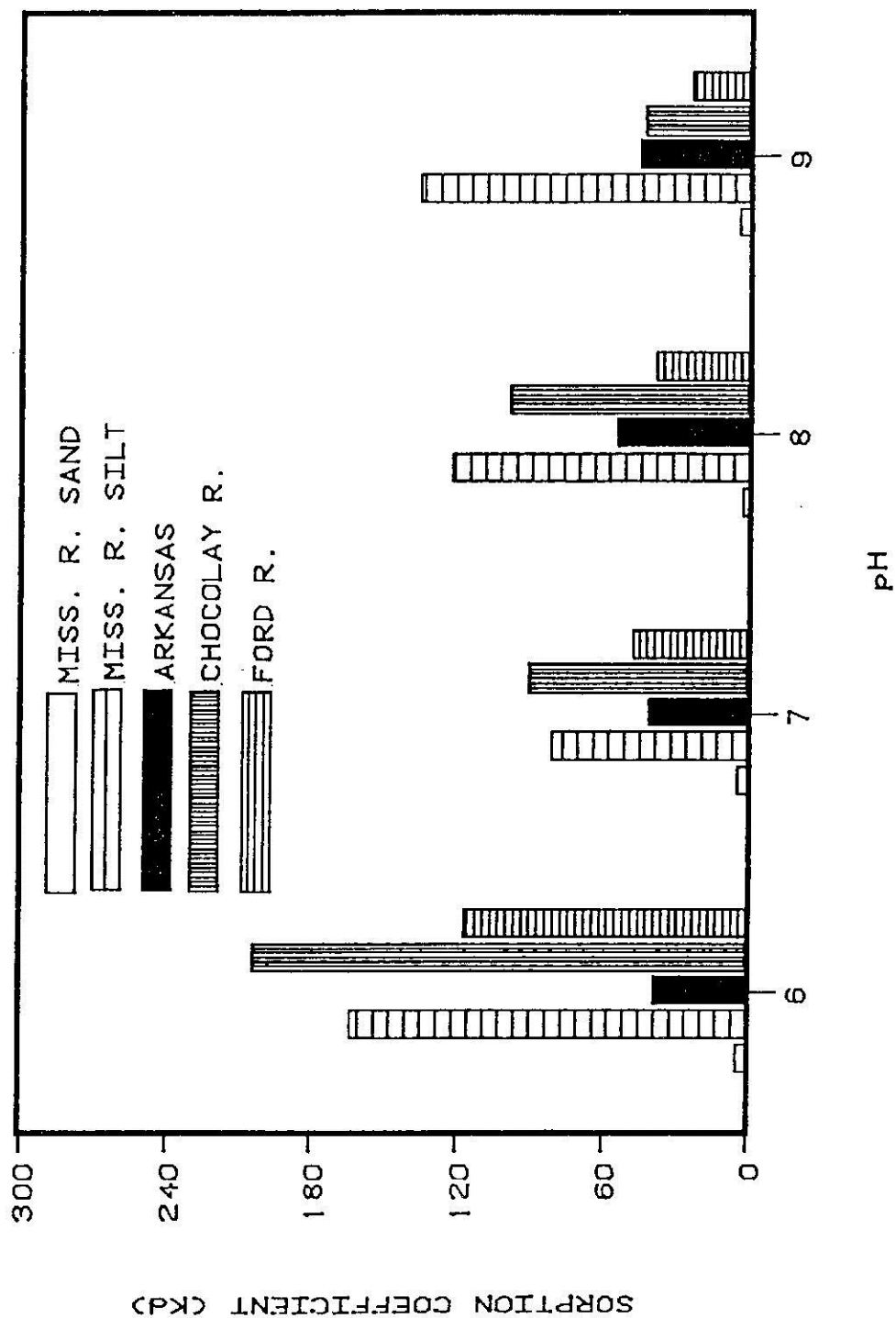


Figure 18. Sorption coefficients (K_d) for ^{14}C -rotenone by five different sediments at four pH's and 20°C.

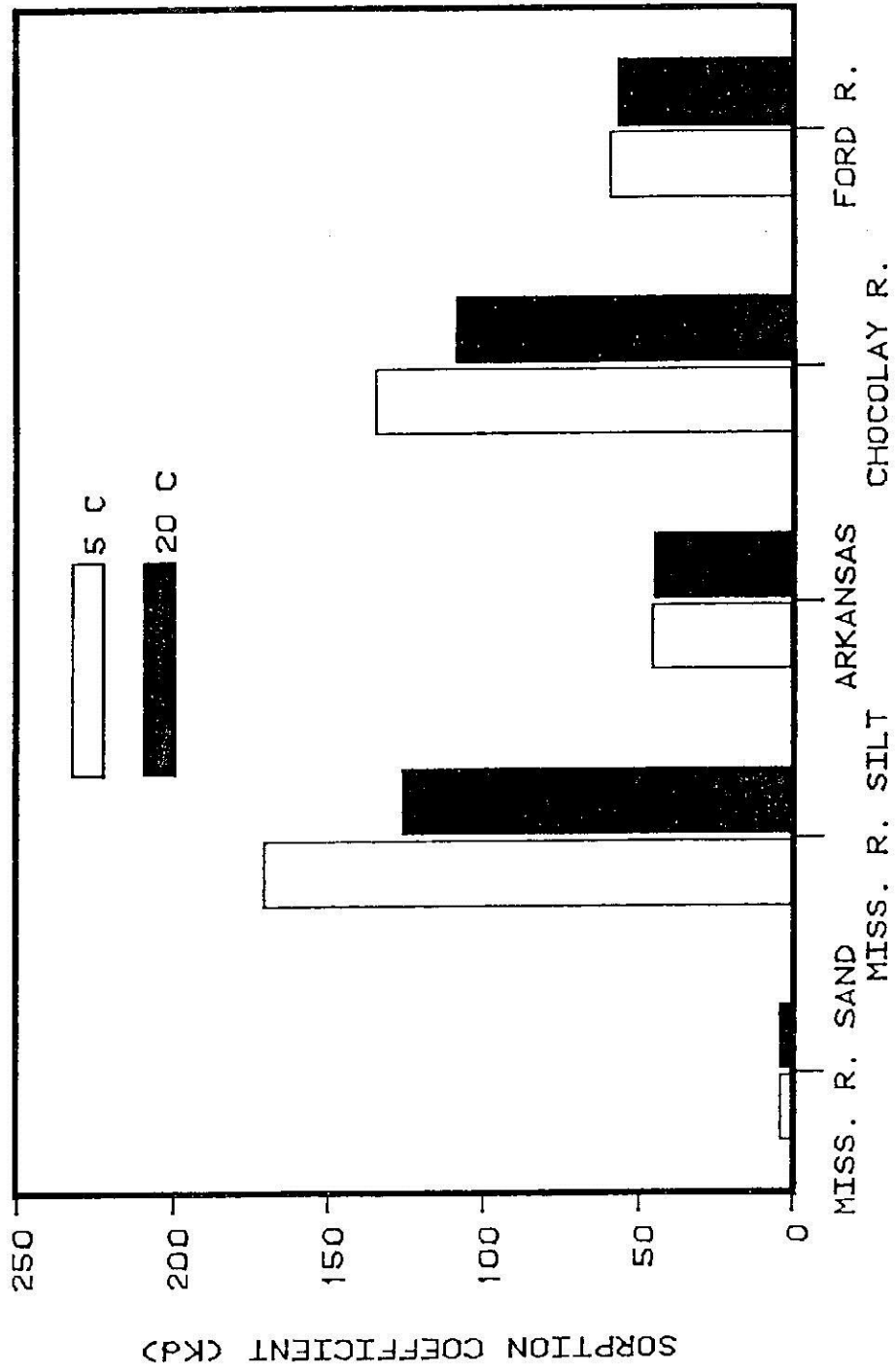


Figure 19. Sorption coefficients (K_d) for ^{14}C -rotenone on bottom sediments at two temperatures.



Figure 20. Desorption (%) of ¹⁴C-rotenone from Mississippi River main channel (River mile 707) sediment at selected temperatures and pH's.

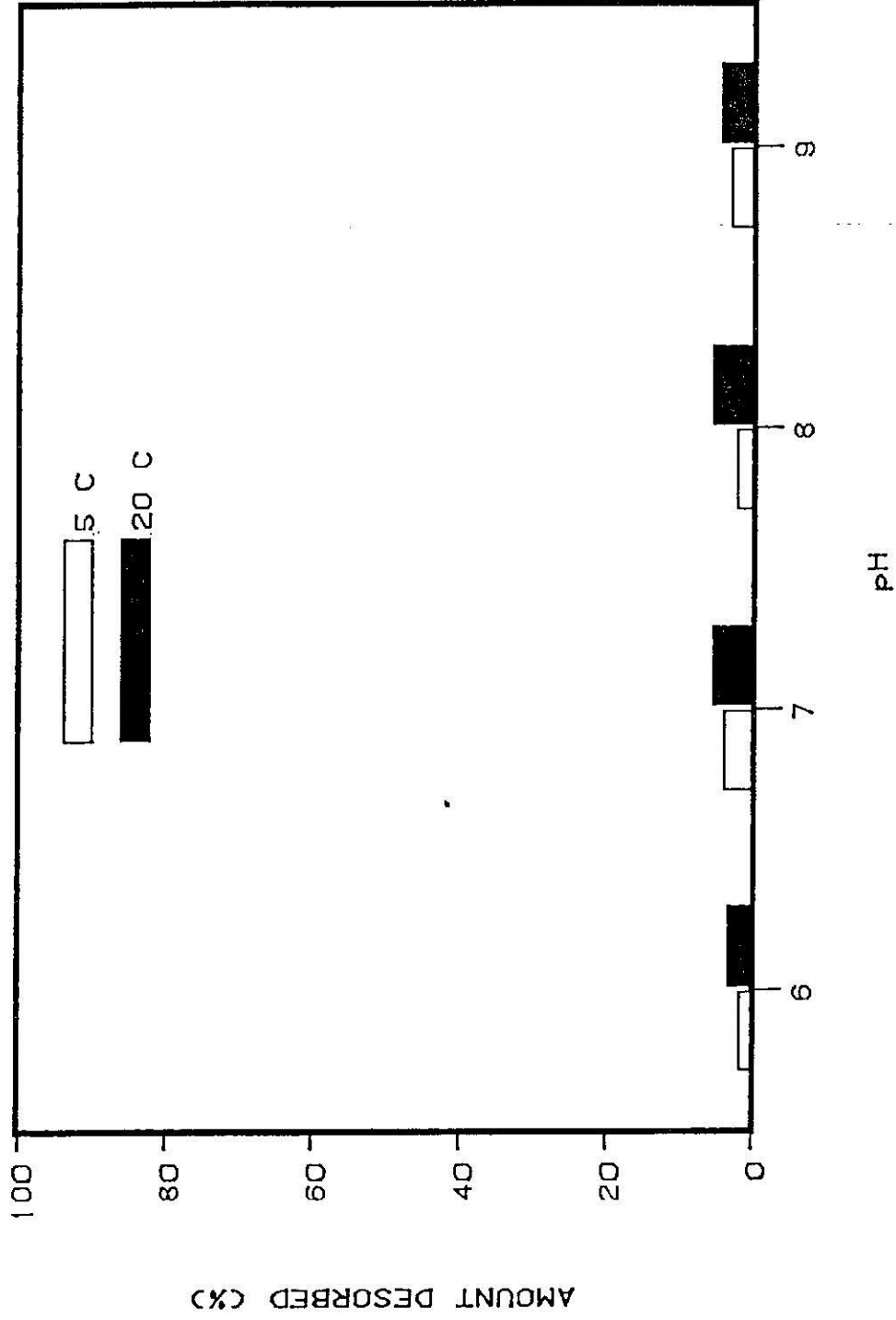


Figure 21. Desorption (%) of adsorbed ^{14}C -rotenone from Mississippi River backwater (River mile 704) sediments at selected temperatures and pH's.

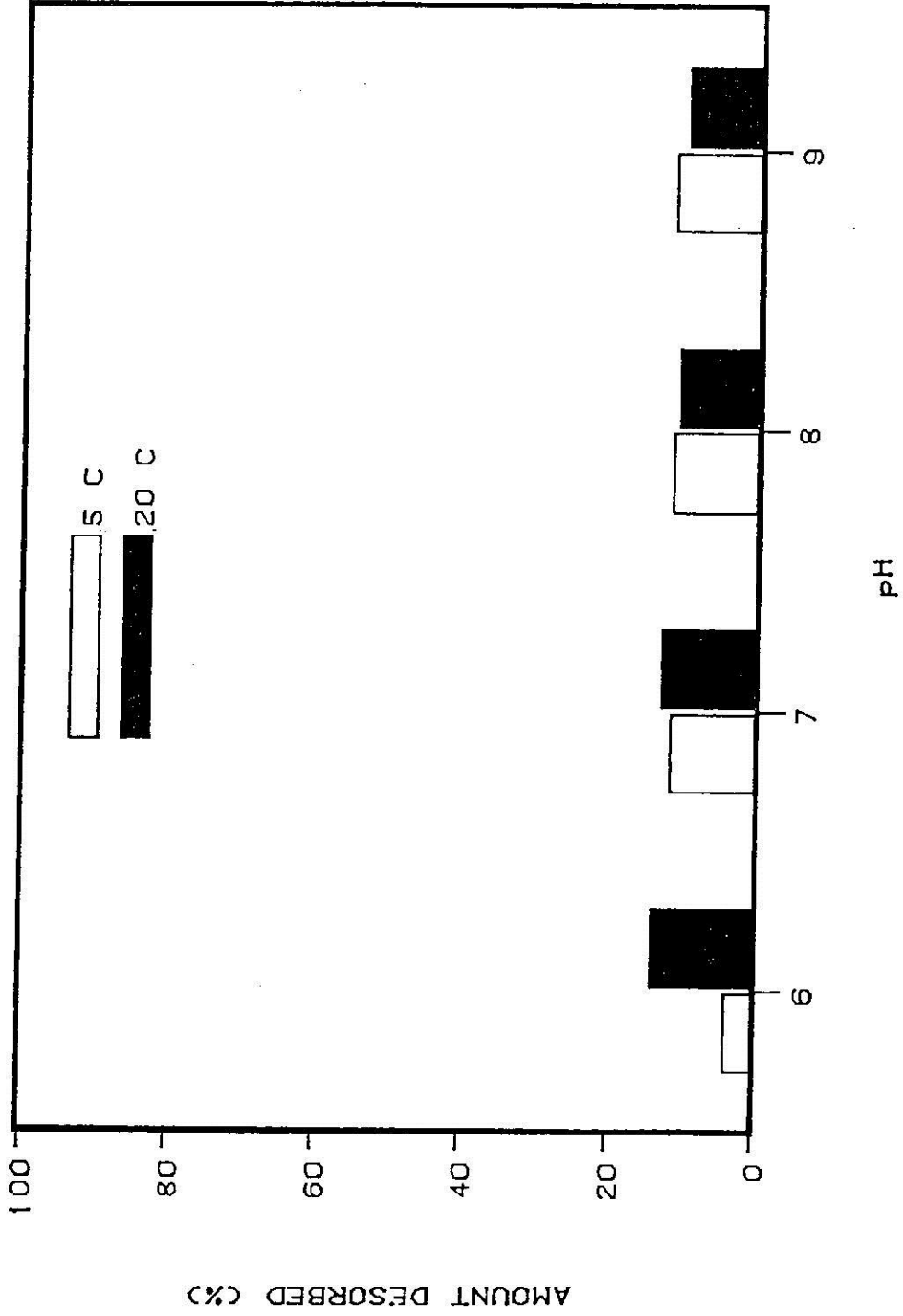


Figure 22. Desorption (%) of adsorbed ¹⁴C-rotenone from Rice Branch Experiment Station, Arkansas, sediments at selected temperatures and pH's.

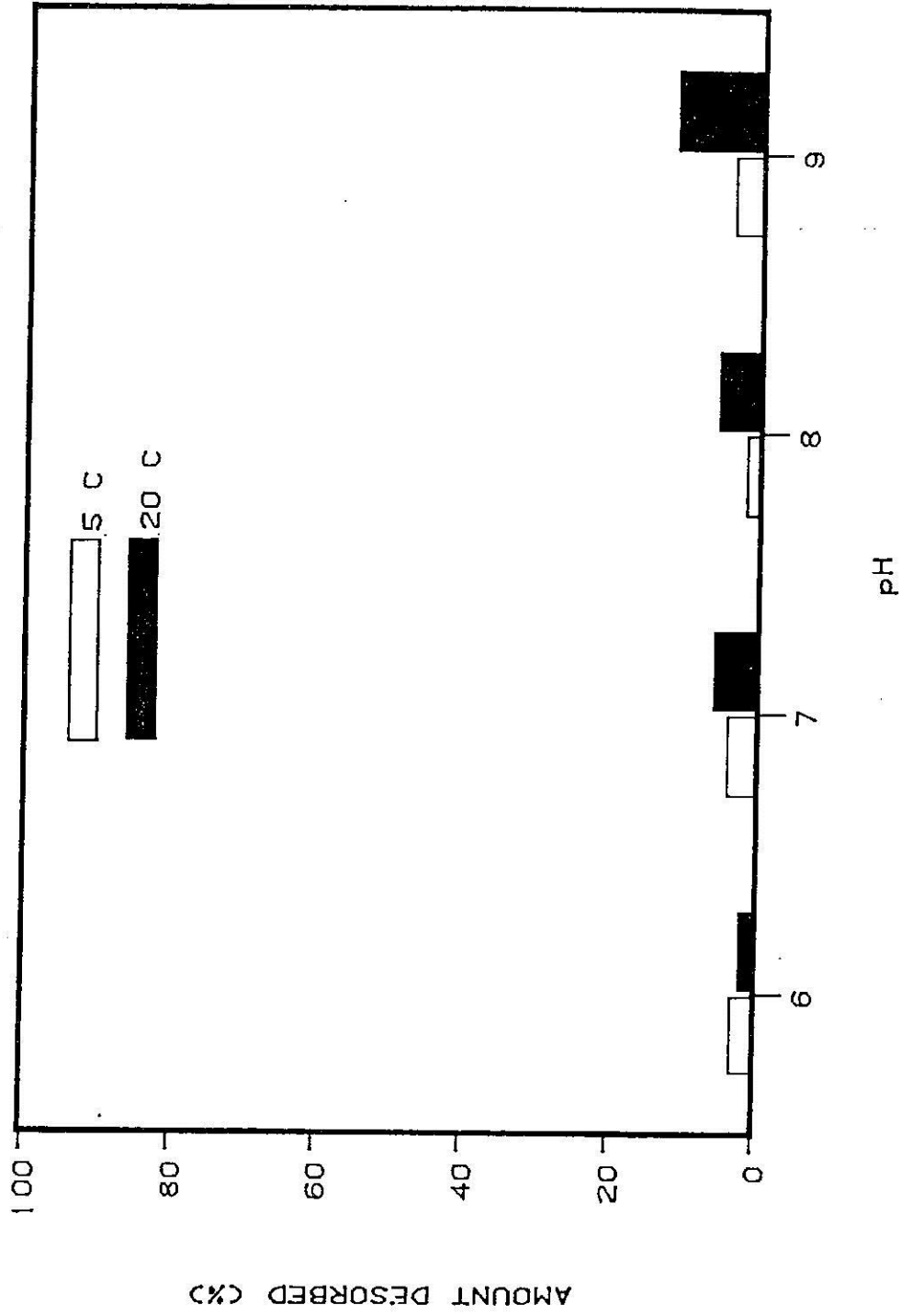


Figure 23. Desorption (%) of adsorbed ¹⁴C-rotenone from Chocolay River, Michigan, sediments at selected temperatures and pH's.

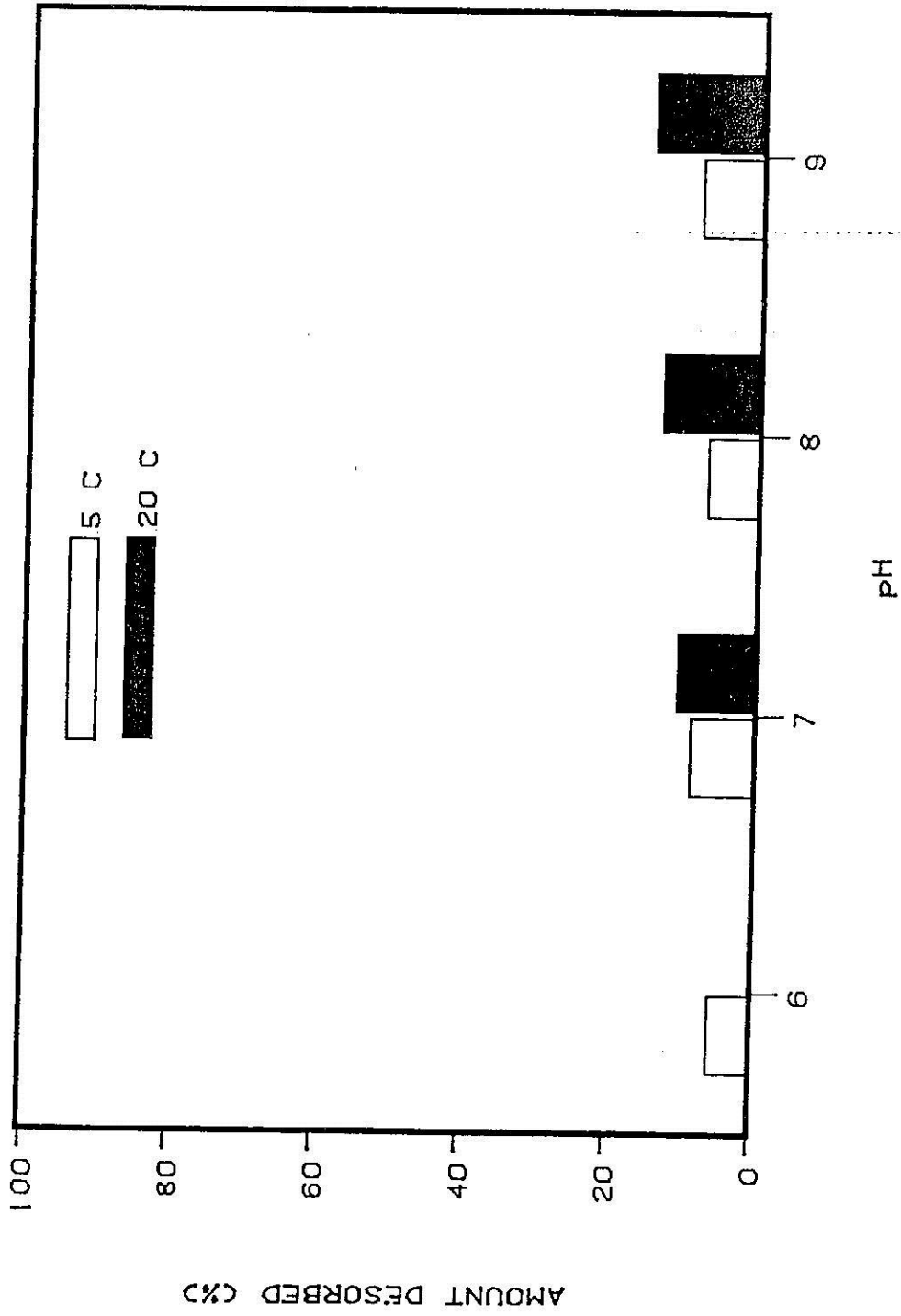


Figure 24. Desorption (%) of adsorbed ^{14}C -rotenone from Ford River, Michigan, sediments at selected temperatures and pH's.